Chemistry & Biology
Article

Selective and Cell-Active Inhibitors of the USP1/UAF1 Deubiquitinase Complex Reverse Cisplatin Resistance in Non-small Cell Lung Cancer Cells

Junjun Chen,[1] Thomas S. Dexheimer,[2] Yongxing Ai,[1] Qin Liang,[1] Mark A. Villamil,[1] James Inglese,[2] David J. Maloney,[2] Ajit Jadhav,[2] Anton Simeonov,[2,*] and Zhihao Zhuang[1,*]
[1]Department of Chemistry and Biochemistry, 214A Drake Hall, University of Delaware, Newark, DE 19716, USA
[2]NIH Chemical Genomics Center, National Human Genome Research Institute, NIH, 9800 Medical Center Drive, MSC 3370, Bethesda, MD 20892-3370, USA
*Correspondence: asimeono@mail.nih.gov (A.S.), zzhuang@udel.edu (Z.Z.)
DOI 10.1016/j.chembiol.2011.08.014

SUMMARY

Ubiquitin-specific proteases (USPs) have in recent years emerged as a promising therapeutic target class. We identified selective small-molecule inhibitors against a deubiquitinase complex, the human USP1/UAF1, through quantitative high throughput screening (qHTS) of a collection of bioactive molecules. The top inhibitors, pimozide and GW7647, inhibited USP1/UAF1 noncompetitively with a K_i of 0.5 and 0.7 μM, respectively, and displayed selectivity against a number of deubiquitinases, deSUMOylase, and cysteine proteases. The USP1/UAF1 inhibitors act synergistically with cisplatin in inhibiting cisplatin-resistant non-small cell lung cancer (NSCLC) cell proliferation. USP1/UAF1 represents a promising target for drug intervention because of its involvement in translesion synthesis and Fanconi anemia pathway important for normal DNA damage response. Our results support USP1/UAF1 as a potential therapeutic target and provide an example of targeting the USP/WD40 repeat protein complex for inhibitor discovery.

INTRODUCTION

Abnormalities in the ubiquitin-mediated processes have been linked to many human diseases, including neurological disorders, viral infection, and cancer. Ubiquitin is a versatile signaling molecule. Although initially discovered in the context of proteasome-mediated protein degradation, ubiquitin and ubiquitin-like proteins are now known to play important roles in a myriad of cellular processes, including membrane trafficking, transcription regulation, and DNA damage response (Kirkin and Dikic, 2007).

In recent years, the ubiquitin-proteasome system has attracted increasing attention as a target for novel therapeutic approaches. A series of proteasome inhibitors has been developed and tested in both cell and animal models (Adams, 2004; Kisselev and Goldberg, 2001). In 2003, the proteasome inhibitor bortezomib (Velcade) was approved by FDA for the treatment of multiple myeloma and later for mantle cell lymphoma. The success of Velcade has established the ubiquitin-proteasome system as a valid target for anti-cancer treatment. However, proteasome inhibitors in general suffer from a narrow therapeutic index because the proteasome is at a convergence point downstream of many important cellular pathways (Guédat and Colland, 2007). A promising alternative to proteasome inhibitor is to target the enzymes upstream of proteasome-mediated protein degradation, i.e., the ubiquitin conjugation and deconjugation system, to generate more specific, less toxic therapeutic agents.

Deubiquitinases (DUBs) are a class of enzymes that cleave the isopeptide bond formed between the C-terminal carboxylate of ubiquitin and a lysine side-chain amino group on the target protein. Besides cleaving the free polyubiquitin chain bearing different linkages, DUB can also remove a single ubiquitin moiety or ubiquitin chain from a target protein (Amerik and Hochstrasser, 2004; Reyes-Turcu et al., 2009). The human genome encodes close to 100 DUBs. DUBs can be classified into five families and ubiquitin-specific proteases (USPs) constitute the largest DUB family (Nijman et al., 2005b). Human USPs are emerging as promising targets for pharmacological intervention. The advantage of inhibiting USPs lies in the potential specificity of therapeutic intervention that can lead to better efficacy and reduce nonspecific side effects.

Close to 60 USPs were identified in humans. However, only a few small-molecule inhibitors have been reported targeting human USPs. Colland et al. (2009) identified a cyano-indenopyrazine derivative that inhibits USP7 with a submicromolar IC_{50}. This compound inhibited deubiquitination of p53 both in vitro and in vivo. Tian et al. (2011) reported another USP7 inhibitor with IC_{50} of 7.8–8.6 μM. Lee et al. (2010) recently reported a USP14 inhibitor with a 4–5 μM IC_{50}, that accelerates protein degradation by inhibiting the proteasome-associated USP14 activity in a reconstituted assay and in mouse embryonic fibroblast cells.

Among the human USPs, USP1 occupies a special position as it is implicated in DNA damage response. Previous studies showed that disruption of USP1 in chicken DT40 cells resulted in increased sensitivity to DNA crosslinkers (Oestergaard et al., 2007). Knockout of the murine USP1 gene in a mouse model resulted in hypersensitivity to mitomycin C (Kim et al., 2009). These observations suggest that inhibiting the cellular activity of USP1 may sensitize cells to DNA crosslinking agents. USP1

has been shown to deubiquitinate PCNA and FANCD2 in cells (Huang et al., 2006; Nijman et al., 2005a). PCNA ubiquitination is central to the normal DNA damage response process in eukaryotes (Bergink and Jentsch, 2009). Monoubiquitination of PCNA is essential for translesion synthesis that promotes lesion-bypass synthesis across the damaged base (Kannouche et al., 2004; Zhuang et al., 2008). Genetic deficiency in the translesion synthesis DNA polymerase η has been linked to the variant form of xeroderma pigmentosum (XPV). FANCD2 is an important protein in the human Fanconi anemia (FA) pathway. Genetic deficiency of FA proteins causes chromosomal instability and predisposition to cancer (Patel and Joenje, 2007). One hallmark of FA patients is the hypersensitivity to DNA cross-linking agents, such as mitomycin C, diepoxybutane, and cisplatin. Eight FA proteins are known to form a multisubunit complex that ubiquitinates FANCD2, which is essential for the repair of DNA interstrand crosslinks (Alpi and Patel, 2009). Because USP1 plays important roles in the two essential DNA damage response pathways, it represents a promising target for small molecule intervention to improve the efficacy of the commonly used DNA damaging drugs by modulating cells' ability of repairing or tolerating DNA lesions.

USP1 belongs to a class of DUBs that require an interacting partner protein for normal enzymatic function (Reyes-Turcu et al., 2009). Human USP1 forms a stable complex with UAF1 (Cohn et al., 2007). USP1 alone possesses low level of deubiquitinating activity. Upon formation of a USP1/UAF1 complex, the catalytic activity of USP1 is greatly stimulated. Given that many USPs exist and function as a complex in vivo (Sowa et al., 2009), it has become imperative to identify inhibitors against the corresponding USP complexes. The different binding partners of USPs could potentially provide the desired selectivity against a large family of USPs that shares an otherwise conserved catalytic site. In this study, we subjected the human USP1/UAF1 complex to high-throughput screening and identified potent and selective inhibitors against USP1/UAF1. The best compounds inhibit USP1/UAF1 through a noncompetitive mechanism with submicromolar K_i values. We also demonstrated that the USP1/UAF1 inhibitors reverse the chemoresistance of non-small cell lung cancer cells to the DNA crosslinker, cisplatin. Our findings support USP1/UAF1 as a potential target for novel anticancer therapy and provide useful chemical tools for understanding the role of deubiquitination in translesion synthesis and Fanconi anemia pathway.

RESULTS

qHTS against USP1/UAF1 Using Ub-Rho as a Substrate

To date, ubiquitin-7-amino-4-methylcoumarin (Ub-AMC) has been the substrate of choice for most DUB high-throughput screening efforts (Colland et al., 2009; Lee et al., 2010). However, coumarin-based fluorescence assays are limited by unfavorable spectroscopic properties, which can lead to fluorescence artifacts from test compounds (Simeonov et al., 2008). To alleviate some of the assay interference arising from fluorescent compounds, we utilized the recently developed ubiquitin-rhodamine110-glycine (Ub-Rho), which exhibits red-shifted fluorescence compared with Ub-AMC, as a substrate (Hassiepen et al., 2007) (Figure 1A). For high-throughput screening, we used the

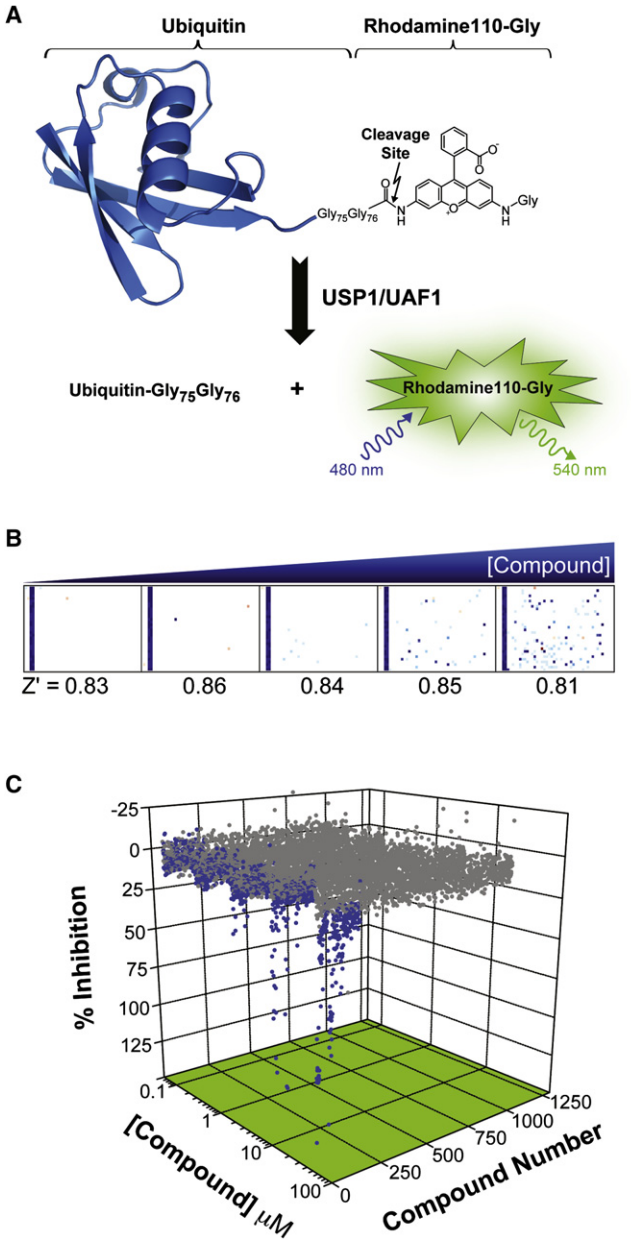

Figure 1. qHTS against Human USP1/UAF1

(A) Schematic representation of the USP1/UAF1-catalyzed hydrolysis of ubiquitin-rhodamine110-glycine substrate.

(B) Heat maps illustrating the 1536-well plate activity of one representative compound library that was screened from low to high concentrations (left to right) with each plate containing a different compound concentration. The percent activity is depicted as a gradient of color where white, blue, and red indicate no, increasing, and decreasing activity, respectively, relative to no-inhibitor control wells. Calculated Z′-values, the standard statistical parameter for evaluating HTS methods, are indicated below each plate.

(C) A three-dimensional scatter plot of the concentration-response curves obtained from the library shown in (B). Percent inhibition was computed from the no-inhibitor (0% inhibited) control and the no-enzyme (100% inhibited) control. Concentration-response relationships are shown for inactive and active compounds in gray and blue, respectively.

See also Table S1.

Table 1. The IC_{50} (μM) Value of the Top Five Compounds in Inhibiting Human USPs Determined Using K63-Linked Diubiquitin Substrate

Compound	Structure	USP1/UAF1	USP7	USP2	USP5	USP8	USP46/UAF1
Pimozide	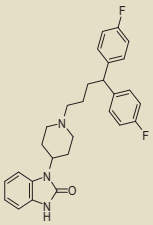	2	47	NI	NI	NI	NI
GW7647	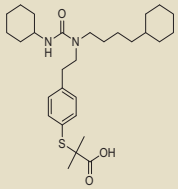	5	44	>114	NI	NI	12
Flupenthixol	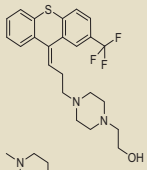	7	13	NI	NI	>114	NI
Trifluoperazine	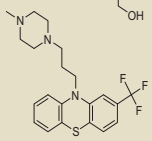	8	9	NI	NI	NI	NI
Rottlerin	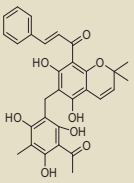	8	13	34	>114	6	15

NI, no significant inhibition was observed at the highest inhibitor concentration of 114 μM.

recombinant USP1/UAF1 complex in a 4 μl assay volume to screen several libraries of 9525 bioactive small molecules in qHTS mode, by testing each compound as a dilution series spanning the concentration range of 0.46–114 μM (see Experimental Procedures) (Inglese et al., 2006). Consistently high Z′ factors (above 0.8) were observed throughout the screen, indicating a robust assay performance (Figure 1B) (Zhang et al., 1999). The screen yielded a range of active compounds associated with different potencies (IC_{50}) and concentration-response curve quality (see Figure 1C for a representative qHTS data set and see Table S1, available online, for the top active compounds).

Secondary Validation of Active Compounds Using an Orthogonal Diubiquitin Cleavage Assay

To validate the top actives using a more physiologically relevant substrate, as well as to rule out false-positives acting via fluorescence interference, we developed an orthogonal gel-based assay using diubiquitin (di-Ub) as a substrate to evaluate the potency of the inhibitors. Diubiquitin as a substrate has been used to characterize the deubiquitinating activity of DUBs from several families (Amerik et al., 1997; Bremm et al., 2010; Cooper et al., 2010; Sato et al., 2008; Virdee et al., 2010). We obtained quantitative kinetic data of USP1/UAF1 hydrolyzing K63- and K48-linked diubiquitin using the gel-based assay. We found that USP1/UAF1 cleaves K63-linked di-Ub substrate with 5.5-fold higher efficiency than K48-linked di-Ub as judged from the k_{cat}/K_m value (0.011 μM^{-1} s^{-1} for K63-linked di-Ub; 0.002 μM^{-1} s^{-1} for K48-linked di-Ub). The kinetic values obtained are comparable to those previously determined for several other DUBs (Cooper et al., 2010; Virdee et al., 2010). We thus chose K63-linked di-Ub as the substrate for quantitative secondary assay analysis.

Using this gel assay, we independently determined the IC_{50} values of the top active compounds inhibiting USP1/UAF1-catalyzed cleavage of the K63-linked di-Ub (Table S1). Out of the 42 compounds tested, five compounds with IC_{50} values ranging from 2 to 8 μM were selected for further studies based on potency and known compound properties (Table 1). Among

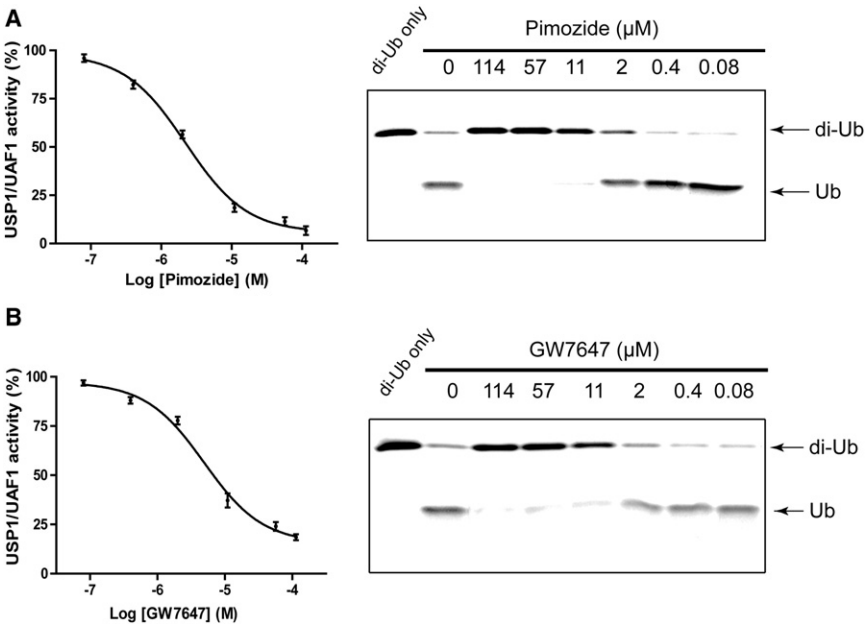

Figure 2. Inhibition of USP1/UAF1 in an Orthogonal Gel-Based Diubiquitin Assay
Dose-dependent inhibition of USP1/UAF1 activity (left) and SDS-PAGE analysis of the cleavage of K63-linked diubiquitin (right) in the presence of different concentrations of pimozide (A) and GW7647 (B).
See also Figure S1.

them, pimozide and GW7647 were the most potent inhibitors displaying concentration-dependent inhibition of di-Ub cleavage with IC_{50} values of 2 and 5 μM, respectively (Figure 2). Three other compounds, flupenthixol, trifluoperazine, and rottlerin, also demonstrated potent inhibition against USP1/UAF1 with IC_{50} values 8 μM or less. While the IC_{50} values determined using di-Ub substrate were generally smaller compared with those determined using Ub-Rho as a substrate, a good correlation between the rank orders determined using the two substrates was noted for the top active compounds.

Selectivity of the USP1/UAF1 Inhibitors against Human USPs

We then determined the selectivity of the five compounds in inhibiting human USPs. We selected the four well studied human USPs, i.e., USP7, USP2, USP5, and USP8, and used them in the diubiquitin cleavage assay. Based on the measured IC_{50} using K63-linked di-Ub substrate (Table 1; Figure S1), we found that pimozide and GW7647 are highly selective against USP1/UAF1. Pimozide inhibits USP7 with an IC_{50} of 47 μM, 24-fold higher than that measured for USP1/UAF1. No inhibition was observed against USP2, USP5, and USP8, even with the highest inhibitor concentration tested (114 μM). GW7647 also showed good selectivity against USP1/UAF1. The IC_{50} determined for USP7 and USP2 (44 and >114 μM, respectively) are 9 and more than 23-fold higher than that determined for USP1/UAF1. Moreover, GW7647 did not inhibit USP5 and USP8. In contrast, flupenthixol and trifluoperazine displayed less selectivity against USPs. Both compounds inhibited USP7 with an IC_{50} comparable to that for USP1/UAF1. Nonetheless, no inhibition was observed against USP2 and USP5. The two compounds demonstrated weak or no inhibition against USP8. Among the top five inhibitors, rottlerin was the least selective inhibitor. It inhibits USP1/UAF1, USP7, USP2, and USP8 with IC_{50} ranging from 6 to 34 μM. Inspection of the rottlerin structure revealed that it contains an α, β-unsaturated carbonyl group, a potential Michael acceptor that covalently modifies active site cysteines. It should be noted that the propensity of rottlerin to form aggregates and inactivate enzyme activities has also been described and could explain its general activity across the USPs (McGovern et al., 2003).

We also tested the top five compounds in inhibiting USP1 alone. In the absence of the UAF1 subunit, USP1 is a poor enzyme and little activity was detected in the cleavage reaction of the K63-linked di-Ub substrate, rendering the inhibition measurement impossible. Thus, we used Ub-Rho as a substrate to assess the inhibition of USP1. Pimozide, GW7647, flupenthixol and trifluoperazine demonstrated low level of inhibition against USP1 alone. The estimated IC_{50} were at least 7- to 14-fold greater compared with the corresponding USP1/UAF1 IC_{50} values determined using Ub-Rho as a substrate (Table S2).

Similar to USP1, human USP46 forms a complex with UAF1 and the activity of USP46 is stimulated by UAF1 (Cohn et al., 2009). Using K63-linked diubiquitin substrate, we assessed the inhibition of USP46/UAF1 by the USP1/UAF1 inhibitors. Pimozide, flupenthixol and trifluoperazine did not inhibit USP46/UAF1 at the highest inhibitor concentrations tested (114 μM), while low level of inhibition by GW7647 was observed (IC_{50} = 12 μM, Table 1).

Selectivity of the USP1/UAF1 Inhibitors against the UCH-Family DUBs and Other Cysteine Proteases

In addition to USPs, we also assessed the selectivity of the top five compounds in inhibiting DUBs from the ubiquitin C-terminal hydrolase (UCH) family. Both human UCH-L1 and UCH-L3 were tested in the inhibition assay. Because UCHs do not cleave the diubiquitin substrate, we used Ub-Rho as a substrate for IC_{50} determination (Table S2). Pimozide, flupenthixol and trifluoperazine were poor inhibitors of UCH-L1 and UCH-L3 (IC_{50} > 500 μM). Similarly, GW7647 inhibited both UCHs with estimated IC_{50} of greater than 200 μM. We also assessed the inhibition of a deSUMOylase, SENP1, by the top five inhibitors using SUMO1-AMC as a substrate. As summarized in Table S2, pimozide, GW7647, flupenthixol, and trifluoperazine showed low level of inhibition against SENP1.

The five prioritized compounds were further tested against unrelated cysteine proteases, including human caspases and papain (Table S2). Pimozide, flupenthixol, and trifluoperazine showed poor inhibition of caspase-1, caspase-3, and caspase-6

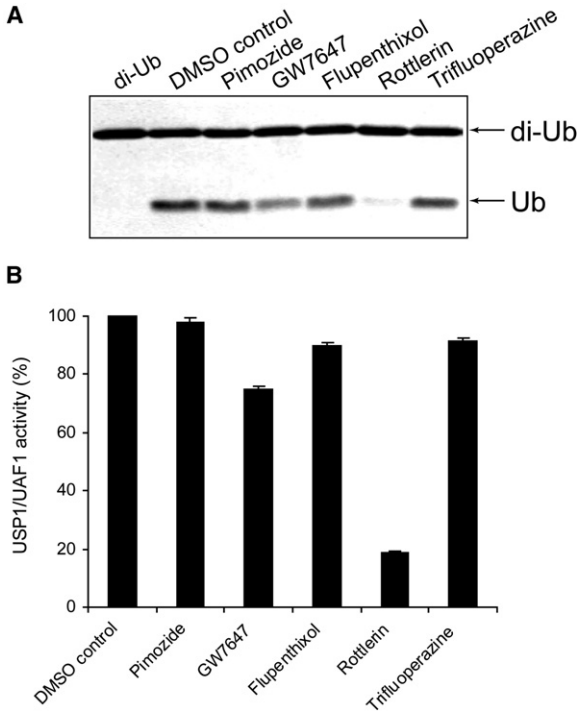

Figure 3. Reversibility of Inhibition by USP1/UAF1 Inhibitors

(A) SDS-PAGE showing the diubiquitin cleavage by USP1/UAF1 that was preincubated with different inhibitors and then rapidly diluted into assay buffer. (B) The remaining activity of USP1/UAF1 treated with five inhibitors. The bar graph represents mean of three independent experiments ±SD. Pimozide, GW7647, flupenthixol, and trifluoperazine are reversible inhibitors. Rottlerin is largely an irreversible inhibitor.

(IC_{50} > 250 μM). GW7647 was also a poor inhibitor of caspase-3 (IC_{50} > 250 μM), but inhibited caspase-1 and caspase-6 with IC_{50} values of 42 μM and 21 μM, respectively. Pimozide and flupenthixol did not inhibit papain (IC_{50} > 250 μM). GW7647 and trifluoperazine demonstrated weak inhibition against papain with IC_{50} values around 130 μM. In comparison, rottlerin inhibited all three caspases, as well as papain with an effect similar to that displayed against the USPs (IC_{50} ranging between 5 and 45 μM).

Reversible USP1/UAF1 Inhibitors

Reversibility of the inhibition of USP1/UAF1 by the top five compounds was tested using a protocol developed by Copeland and coworkers (Copeland, 2005). USP1/UAF1 (10 μM) was incubated with the compound applied at a concentration ten times its IC_{50}. Upon rapid dilution (100-fold) into the assay buffer, the incubated USP1/UAF1-inhibitor mixture was assayed for enzymatic activity. Our results indicated that pimozide, GW7647, flupenthixol, and trifluoperazine were largely reversible inhibitors because USP1/UAF1 treated with these inhibitors exhibited rapid recovery of activity upon dilution. The measured activity of USP1/UAF1 following dilution was close to that determined in the control reaction using DMSO solvent (Figure 3). In contrast, rottlerin was an irreversible inhibitor of USP1/UAF1 with only 18% enzymatic activity recovered following the same incubation-dilution protocol.

Pimozide and GW7647 Inhibit USP1/UAF1 by a Noncompetitive Mechanism

The inhibition mechanism of pimozide and GW7647 was assessed by measuring the steady-state rate constants at varied inhibitor concentrations using K63-linked di-Ub as a substrate. The Lineweaver-Burk plots for both pimozide and GW7647 (Figure 4) indicate a noncompetitive inhibition mechanism. The measured inhibition constants (K_i) for pimozide and GW7647 are 0.5 and 0.7 μM, respectively. These observations suggest that both pimozide and GW7647 bind at a site other than the active site of USP1/UAF1. We can also infer that both inhibitors bind the enzyme and enzyme substrate complex with equal affinity. We ruled out that pimozide and GW7647 inhibited USP1/UAF1 by disrupting the protein-protein interaction within the complex. Our native gel electrophoresis following the incubation of USP1/UAF1 with pimozide or GW7647 (up to 10 × IC_{50}) showed no dissociation of the USP1/UAF1 complex (Figure S2).

USP1/UAF1 Inhibitors Sensitize Cisplatin-Resistant NSCLC Cells to Cisplatin Killing

We determined the viability of the cisplatin-resistant human non-small cell lung cancer (NSCLC) cells (H596, NCI) treated with a combination of cisplatin and the USP1/UAF1 inhibitors, pimozide or GW7647. Cisplatin alone killed human H596 cells with an EC_{50} of 8.1 μM (Figures 5A and 5B), in concordance with a previous report (Zeng-Rong et al., 1995). Pimozide and GW7647 alone demonstrated modest cytotoxicity against H596 cells with EC_{50} of 21 and 26 μM, respectively. We then assessed the cytotoxicity of cisplatin in combination with USP1/UAF1 inhibitors by following the method of Chou-Talalay (Chou et al., 1994; Zastre et al., 2007). Specifically, we measured the viability of NCI H596 cells treated with a combination of cisplatin and USP1/UAF1 inhibitor (pimozide or GW7647) at a fixed molar ratio of 1:1 or 1:4 (Figures 5A and 5B). EC_{50} were obtained for each combination. A combination of cisplatin and pimozide at a ratio of 1:1 and 1:4 significantly enhanced the cytotoxicity of cisplatin as judged from the EC_{50} values of 5.1 and 2.8 μM, respectively. For the cisplatin and pimozide combination at a ratio of 1:4, the EC_{50} of 2.8 μM approaches the EC_{50} of 1.2 μM determined for the cisplatin-sensitive NSCLC H460 cell line (Figures S3A and S3B). Enhanced cytotoxicity was also observed for H596 cells treated with a combination of cisplatin and GW7647 at a ratio of 1:4 with a measured EC_{50} of 4.3 μM.

We next determined the nature of the interactions between cisplatin and the USP1/UAF1 inhibitors. To this end, the cell killing curves were analyzed using the program CalcuSyn as described previously (Chou, 2010; Radujkovic et al., 2005; Shanks et al., 2005; Zastre et al., 2007). The resulting combination indexes (CI) were plotted against the fraction affected by the dose (Fa). A combination index (CI) smaller than one indicates synergistic effect, while a CI equal to one indicates additive effect (Chou, 2010). As shown in Figure 5C, a synergistic effect was observed for the combination of cisplatin and pimozide at a ratio of 1:1 and 1:4, and for cisplatin and GW7647 at a ratio of 1:4.

We also tested the cisplatin-sensitive human non-small cell lung cancer (NSCLC) cells (H460, NCI). Interestingly, a combination of cisplatin and pimozide/GW7647 at a ratio of 1:1 and 1:4 did not further increase the cytotoxicity of cisplatin (Figures S3A and S3B).

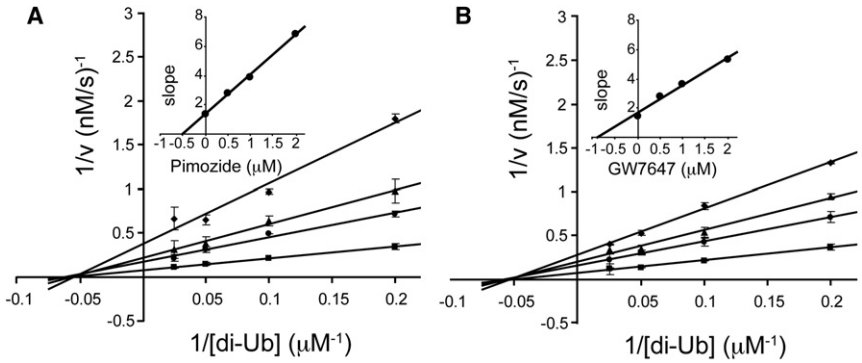

Figure 4. Inhibition Mechanism of Pimozide and GW7647

Lineweaver-Burk plots of USP1/UAF1-catalyzed hydrolysis of diubiquitin in the presence of 0 (square), 0.5 (circle), 1 (triangle), 2 (diamond) μM of pimozide (A) or GW7647 (B). The inset shows the plot of the slopes obtained from the Lineweaver-Burk plots against the inhibitor concentrations.

See also Figure S2.

Pimozide and GW7647 Inactivate USP1/UAF1 in Cells

USP1/UAF1 was shown to deubiquitinate both PCNA and FANCD2 in response to DNA damage (Cohn et al., 2007; Huang et al., 2006). In order to demonstrate that pimozide and GW7647 inhibit the USP1/UAF1 activity in cells, we developed an assay to determine the levels of Ub-PCNA or Ub-FANCD2 in cells treated

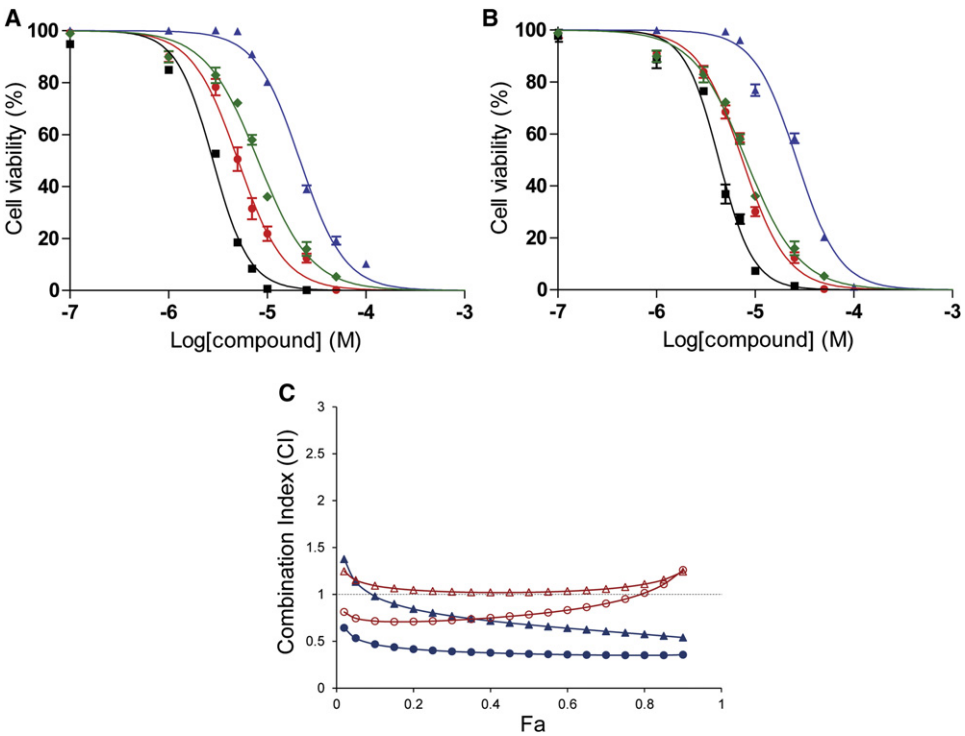

Figure 5. Cytotoxicity of Cisplatin, Pimozide, and GW7647 Tested as a Single Agent or in Combination on Cisplatin-Resistant NSCLC Cells (H596)

(A) Cytotoxicity of cisplatin alone (green diamond), pimozide (blue triangle), or a combination of cisplatin and pimozide at ratios of 1:1 (red circle), 1:4 (black square).

(B) Cytotoxicity of cisplatin alone (green diamond), GW7647 (blue triangle), or a combination of cisplatin and GW7647 at ratios of 1:1 (red circle), 1:4 (black square). Cell viability determined with equal volume of vehicle was treated as 100%. Data are mean of three independent experiments ±SD.

(C) Combination index (CI) for treating H596 cells with a combination of cisplatin and pimozide or GW7647. Cells were treated with a combination of cisplatin and pimozide at ratios of 1:1 (filled blue triangle), 1:4 (filled blue circle) or with a combination of cisplatin and GW7647 at ratios of 1:1 (open red triangle), 1:4 (open red circle). The combination indices were calculated using software CalcuSyn for each combination and plotted against the fraction of cells affected (Fa). The dashed horizontal line in the figure represents a combination index = 1. See also Figure S3.

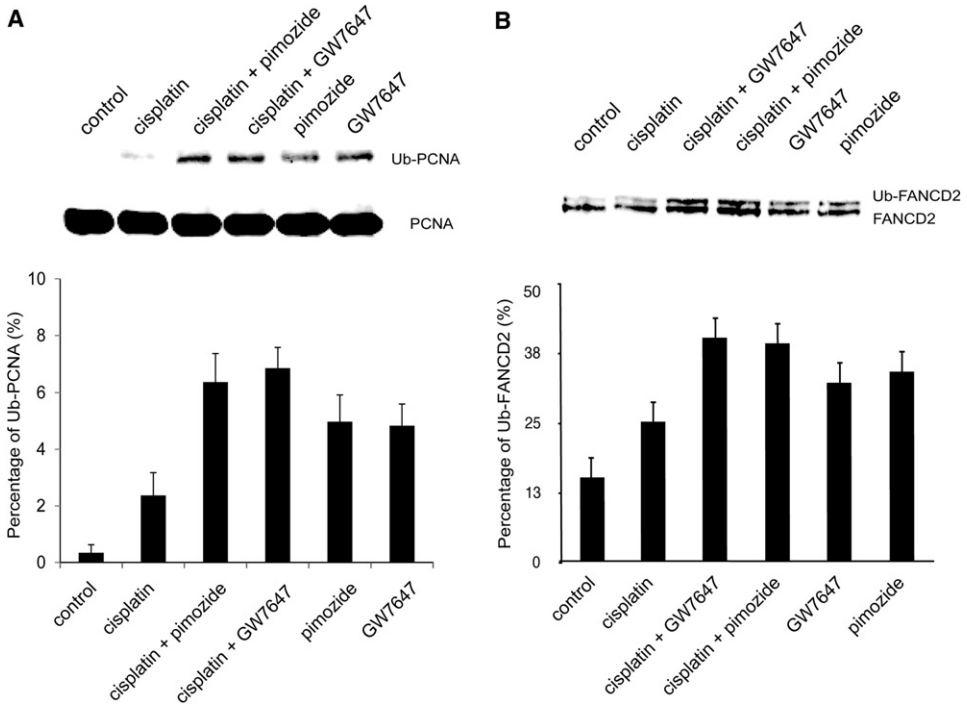

Figure 6. Treatment of Human Cells by USP1/UAF1 Inhibitors Leads to the Increase in PCNA and FANCD2 Monoubiquitination

HEK293T cells were treated with cisplatin, USP1/UAF1 inhibitors (pimozide or GW7647), or a combination of cisplatin and pimozide or GW7647. The cells treated with the vehicle (DMSO) were used as control. Cell lysate was analyzed by western blotting using anti-PCNA antibody (A) or anti-FANCD2 antibody (B). The PCNA and Ub-PCNA bands were quantified and the percentage of monoubiquitinated PCNA is reported in the bottom panel. The data presented here were an average of three independent experiments. The percentage of monoubiquitinated FANCD2 was determined in the same way. See also Figure S4.

with cisplatin, pimozide/GW7647 or a combination of cisplatin and pimozide/GW7647. When HEK293T cells were treated with cisplatin alone, a small, but significant, percent of Ub-PCNA was detected, agreeing with observations made in several different human cell lines (Albertella et al., 2005; Brun et al., 2010; Terai et al., 2010). When the cells were incubated with a combination of cisplatin with pimozide or GW7647, the percentage of Ub-PCNA more than tripled (Figure 6A). Notably, when the cells were treated with pimozide or GW7647 alone, a significant increase in monoubiquitination of PCNA was also observed, albeit the increase was lower than that of the cells treated with cisplatin in combination with pimozide or GW7647. Similar observation was also made for the cisplatin-resistant and -sensitive NSCLC cells (Figures S4A and S4B).

We also assessed the effect of USP1/UAF1 inhibitors on the cellular Ub-FANCD2 level in HEK293T cells. Using an anti-FANCD2 antibody, we observed that approximately 25% of FANCD2 were monoubiquitinated when cells were treated with cisplatin alone. Similar to PCNA monoubiquitination, treatment of HEK293T cells with cisplatin in combination with pimozide or GW7647 led to increase in the level of monoubiquitinated FANCD2 to 40%. Treatment of HEK293T cells with pimozide or GW7647 led to increase in Ub-FANCD2 level, but to an extent lower than that of the cells treated with the combination of cisplatin with pimozide or GW7647.

We further investigated the effect of pimozide and GW7647 on histone H2A monoubiquitination, a prevalent histone modification in mammalian cells. Treating the HEK293T cells with pimozide or GW7647 had no effect on the level of Ub-H2A either in the presence or absence of cisplatin (Figure S4C).

DISCUSSION

Conventional protease inhibitor discovery relies on small molecules that bind to the protease active site. This approach has garnered some success, especially when structural information of the protease is available. However, it faces challenges due to the common problem of overlapping activity or lack of specificity of the active site-targeting protease inhibitors. In recent years there has been increasing realization that both selectivity and potency of protease inhibitors can be potentially achieved by targeting the protease exosite or allosteric site (Drag and Salvesen, 2010; Kornacker et al., 2005; Scheer et al., 2006).

One emerging feature of DUBs and the related deSUMOylases is that the efficient catalysis requires extensive interactions in the enzyme exosite. This is reflected by the observation that the substrate based on the linear epitope recognized by the active site of DUBs or deSUMOylases can only be cleaved at a rate five to six orders of magnitude lower compared with substrate that contains a complete ubiquitin or SUMO moiety (Drag and Salvesen, 2010). Thus, targeting the DUB exosite is a promising alternative strategy for developing DUB inhibitors. Moreover, many DUBs are regulated by specific interaction with their protein partner (Reyes-Turcu et al., 2009). For some DUBs, this interaction is required for their catalytic activity. Although the detailed mechanism of such regulation remains to be elucidated,

allosteric regulation likely plays a central role in modulating the DUB enzymatic activity. Therefore, inhibitor discovery by targeting DUBs at sites other than the active site should serve to validate the new paradigm of protease inhibitor development. High-throughput screening, being largely a mechanistically unbiased approach, carries an advantage over rational inhibitor design that targets solely the active site, and as such is expected to allow the identification of inhibitors targeting the exosite or allosteric site.

In this study, we identified USP1/UAF1 inhibitors, pimozide and GW7647, through quantitative high-throughput screening against a collection of 9525 bioactive molecules. Our kinetic analyses revealed noncompetitive mechanism for both inhibitors, suggesting that both compounds bind at a site different from the active site. Interestingly, both compounds are poor inhibitors of USP1 alone. This again supports the notion that both inhibitors bind outside the USP1 active site and may form the basis for the selectivity of pimozide and GW7647 in inhibiting USP1/UAF1 among the group of human USPs tested. We also confirmed that pimozide and GW7647 are both reversible inhibitors. Different from a previously reported USP7 inhibitor that acts as an uncompetitive inhibitor (Colland et al., 2009), pimozide and GW7647 appear to bind to both the enzyme-substrate complex and the free enzyme. The inhibition mechanism of another recently reported inhibitor against USP14 has not been rigorously studied, albeit a competitive mechanism was suggested (Lee et al., 2010).

We found that both pimozide and GW7647 were more potent inhibitors against USP1/UAF1 when the inhibition was assayed using K63-linked diubiquitin substrate as compared with Ub-Rho as a substrate. This raised the interesting possibility that the different binding modes of diubiquitin and Ub-Rho to USP1/UAF1 may affect the potency of the noncompetitive inhibitor. Recent structure determination of the K63-linked diubiquitin bound to AMSH-LP revealed specific interactions between the proximal ubiquitin and the DUB catalytic core as well as an inserted motif (Sato et al., 2008). Thus, it is possible that pimozide and GW7647 bind to a site on USP1/UAF1 that partially overlaps with the proximal ubiquitin binding site, thus contributing to the stronger inhibition observed for diubiquitin as a substrate. Another possibility is that pimozide and GW7647 may bind to an allosteric site that influences the binding of proximal ubiquitin. It should be noted that we used K63-linked di-Ub as a substrate for selectivity assay because USP1/UAF1 cleaves K63-linked di-Ub more efficiently than K48-linked di-Ub. However, we do not rule out that the identified inhibitors may inhibit USPs with varied potency when a ubiquitin chain with different linkages is tested as a substrate.

Many anticancer drugs are DNA crosslinkers that exert their effects by damaging the genomic DNA of cancer cells, which in turn triggers apoptosis of the cells. Cisplatin and other platinum-based anticancer drugs act by crosslinking the genomic DNA. Despite considerable success in treating human cancers, the effectiveness of cisplatin and other platinum drugs in clinics has been limited by the resistance that cancer cells developed during the course of therapy. Therefore, overcoming cancer cells' resistance to cisplatin and other platinum drugs by combination therapies is a promising strategy for treating cancer. Cisplatin is known to elicit both intrastrand and interstrand DNA crosslinks, with the intrastrand crosslink being more prevalent. Previous studies have linked the Fanconi anemia pathway to cellular repair of interstrand DNA crosslinks caused by chemical crosslinker such as cisplatin, albeit the exact mechanism of this repair process remains to be fully elucidated (Wang, 2007). On the other hand, translesion synthesis has been linked to cell's ability to tolerate both cisplatin-induced intrastrand and interstrand DNA crosslinks (Hicks et al., 2010; Sonoda et al., 2003; Wu et al., 2004). Furthermore, translesion synthesis and Fanconi anemia pathway are closely linked. Recent studies revealed that K164 PCNA monoubiquitination is required to recruit FANCL to the chromatin structure and stimulate FANCL-catalyzed ubiquitination of FANCD2 and FANCI (Geng et al., 2010).

The exact role of deubiquitination of PCNA and FANCD2 by USP1/UAF1 in human DNA damage response remains to be elucidated. Knocking down USP1 in human HEK293 cells was shown to protect cells from MMC-induced chromosomal aberrations (Nijman et al., 2005a). Nonetheless, in chicken DT40 cells, deletion of USP1 led to increased sensitivity of DT40 cells to cisplatin (Oestergaard et al., 2007). Similar observation was made in USP1 knockout mouse (Kim et al., 2009). A unified view of the effect of inhibiting USP1 cellular activity on vertebrate DNA damage response has not been obtained. In the current study, we demonstrated that inhibiting the cellular activity of USP1/UAF1 by small molecule inhibitors sensitized human cisplatin-resistant NSCLC H596 cells to DNA crosslinker cisplatin. We also observed sensitization of H596 cells to cisplatin when treated in combination with siRNA targeting USP1, albeit to a less extent under our assay condition (Figure S3C). Compared with the siRNA approach, the small-molecule inhibitor allowed us to probe the cellular function of USP1/UAF1 without perturbing the level of USP1/UAF1 complex in human cells. This is particularly desirable given the recent realization that a vast interaction network exists between USPs and many of their protein partners in cells (Sowa et al., 2009). Notably, we did not observe further sensitization of cisplatin-sensitive NSCLC H460 cell lines to cisplatin upon treatment with pimozide and GW7647. Our observations support the notion that USP1/UAF1 is involved in the NSCLC cell's resistance to cisplatin-induced DNA damage.

We demonstrated the on-target effect of the USP1/UAF1 inhibitors in human cells in disrupting the USP1-catalyzed deubiquitination of PCNA and FANCD2, but not the deubiquitination of histone H2A. We observed that treatment of cells with the USP1/UAF1 inhibitor alone led to increase in the levels of Ub-PCNA and Ub-FANCD2. This observation suggests that PCNA and FANCD2 undergo dynamic ubiquitination and deubiquitination even in the absence of exogenous DNA damaging events.

The USP1/UAF1 inhibitors identified in this work are bioactive molecules. Pimozide, a diphenylbutylpiperidine derivative, is also known for its neuroleptic property in treating chronic schizophrenic patients (Opler and Feinberg, 1991). However, evidence has suggested that the pharmacological activity of pimozide may not be limited to its neuroleptic function. It has been reported that pimozide inhibits the proliferation of human melanoma and breast cancer cells (Neifeld et al., 1983; Strobl et al., 1990). In this study, we showed that pimozide is a potent inhibitor of a human DUB, USP1/UAF1, and provided insight into the molecular basis for the antineoplastic activity of pimozide. GW7647, another potent USP1/UAF1 inhibitor, was initially

identified as an agonist of human peroxisome proliferator-activated receptor-α (PPARα), a ligand-activated transcription factor involved in the regulation of lipid homeostasis (Brown et al., 2001). So far, no cytocidal activity against human cell lines has been reported for GW7647. Our studies revealed a modest synergistic effect of GW7647 in killing human cisplatin-resistant NCSLC cells when combined with cisplatin. Taken together, the studies presented here revealed the potential new use of two pharmacologically active agents.

A desirable feature of therapeutics to be used in combination with DNA crosslinking drugs is the synergistic interaction between the compound and DNA crosslinkers. The synergy between cisplatin and USP1/UAF1 inhibitors was demonstrated in preventing the proliferation of cisplatin-resistant NSCLC cells. Our results validated USP1/UAF1 as a potential target for developing novel therapeutics for combination therapy to overcome cancer cells' resistance to cisplatin and possibly other DNA crosslinkers.

Lastly USP1/UAF1 represents a group of USPs that were recently found to specifically interact with WD40 repeat proteins (Sowa et al., 2009). The present identification of selective, noncompetitive inhibitors against the USP1/UAF1 complex represents the first example of targeting the USP/WD40 repeat protein complex for inhibitor discovery. The newly identified USP1/UAF1 inhibitors should also serve as valuable chemical tools for studying the human DNA damage response that involves translesion synthesis and Fanconi anemia pathway.

SIGNIFICANCE

In recent years, the noncanonical function of ubiquitin has been shown to be important for a number of cellular processes, including membrane trafficking, innate immunity, kinase signaling, chromatin dynamics, and DNA damage response. Recent discoveries of the essential regulatory roles of ubiquitin in DNA damage response have fueled the rapid progress in this important research area. Two major DNA damage response pathways, namely, translesion synthesis (TLS) and Fanconi anemia (FA), are at the center of the research effort in understanding the novel function of ubiquitin. Moreover, the two pathways also provide promising targets for novel anticancer therapies. USP1/UAF1, as a prototype of a group of USP/WD40 repeat protein complexes, has attracted increasing attention for small-molecule inhibitor discovery. However, no inhibitors of USP1/UAF1 have been reported. The lack of small-molecule inhibitors of ubiquitin-specific proteases (USPs) in general has hampered the progress in understanding and exploiting this large family of DUBs. In this work we discovered potent, and cell-active inhibitors of the USP1/UAF1 complex through quantitative high-throughput screening (qHTS). This work demonstrated the feasibility of selective inhibition of the deubiquitinase complex that belongs to the widespread USP/WD40 repeat protein family. The therapeutic potential of inhibiting USP1/UAF1 was demonstrated by the observation that the USP1/UAF1 inhibitors can reverse the chemoresistance of non-small cell lung cancer cells to the chemotherapeutic agent, cisplatin. The current USP1/UAF1 inhibitors are also valuable chemical tool for understanding the role of deubiquitination in translesion synthesis and Fanconi anemia pathway.

EXPERIMENTAL PROCEDURES

Quantitative High-Throughput Screen

USP1/UAF1 activity was monitored in a fluorometric assay, using ubiquitin-rhodamine110-glycine (Ub-Rho; Boston Biochem). Enzymatic reactions were conducted in an assay buffer (50 mM HEPES [pH 7.8], 0.5 mM EDTA, 100 mM NaCl, 1 mM TCEP, 0.1 mg/ml BSA, and 0.01% Tween-20) that contained 1 nM USP1/UAF1. Each individual compound was tested at five concentrations in the range of 0.46–114 μM. The plates were incubated for 15 min to attain equilibrium, and then the enzymatic reaction was initiated by dispensing 1 μl of Ub-Rho solution (150 nM final concentration). The plates were directly transferred to a ViewLux high-throughput CCD imager (PerkinElmer), where kinetic measurements of rhodamine fluorescence were acquired using a 480 nm excitation/540 nm emission filter set. The change in fluorescence intensity over a 5 min reaction period (typically associated with less than 10% substrate conversion) was normalized against no-inhibitor and no-enzyme controls and the resulting percent inhibition data were fitted to a sigmoidal dose response using a four-parameter Hill equation (Southall et al., 2009).

Assay Inhibition of USP1/UAF1 Using K63-Linked di-Ub as a Substrate

Inhibitors at varied concentrations (0.08–114 μM) were added to the assay solution containing 100 nM USP1/UAF1, 2 μM K63-linked diubiquitin (Boston Biochem) in a buffer containing 50 mM HEPES (pH 7.8), 0.1 mg/ml BSA, 0.5 mM EDTA, and 1 mM DTT. The reaction was allowed for 1 hr at 37°C, and quenched by the addition of Laemmli sample buffer. The reaction product was separated on a 20% denaturing SDS-PAGE gel and stained with Coomassie blue. The intensity of the individual diubiquitin and monoubiquitin bands were quantified using Quantity One software (Bio-Rad). The enzyme activity was normalized against no-inhibitor control and plotted against inhibitor concentration. The IC_{50} value was determined by fitting the dose response curve to Equation 1 using GraphPad Prism (GraphPad Software).

$$Y = Y_0 + \frac{Y_{max} - Y_0}{1 + 10^{X - \mathrm{Log}\ IC_{50}}}$$

where X = Log[inhibitor]; Y is the enzyme activity in percent relative to control. GraphPad Prism reports the standard error of $\mathrm{Log}IC_{50}$, but not of IC_{50}.

Cytotoxicity Assay

Human non-small cell lung cancer (NSCLC) cell line H596 and H460 were purchased from American Type Culture Collection. H596 and H460 cells were grown in RPMI 1640 medium (ATCC) supplemented with 10% FBS (ATCC) at 37°C and 5% CO_2. In cytotoxicity assay, 5×10^3 cells were seeded in each well of the 96-well plate and grown for 24 hr in humidified incubator. H596 and H460 cells were first treated with cisplatin, pimozide or GW7647 individually for 48 hr to determine the EC_{50} of each compound. In combination assay, cisplatin was dissolved in saline solution; pimozide and GW7647 were dissolved in DMSO. Equal volume of above solutions was added to each well and cells were incubated for 48 hr. The cells treated with equal volume of DMSO and saline were used as control and designated as 100% viability. Ten microliters of CCK-8 solution (Dojindo Molecular Technologies) was added to each well following the treatment to determine the cell viability where the tetrazolium salt (WST-8) was reduced by dehydrogenases in cells to give a yellow-colored product (formazan). Plates were incubated for 3 hr at 37°C and the absorbance at 450 nm was measured using a microplate reader (PerkinElmer). Dose-response curves were generated and EC_{50} value was obtained by fitting the data to Equation 2 using GraphPad Prism.

$$Y = \frac{100}{1 + 10^{(Log\ EC_{50} - X) \cdot n}}$$

where X = Log[inhibitor]; Y is cell viability in percent relative to the control; n is Hillslope.

Assessment of the Synergistic Interaction of Cisplatin and the USP1/UAF1 Inhibitor

To determine whether a combination of cisplatin and the USP1/UAF1 inhibitors exert the effect synergistically or additively, cisplatin and USP1/UAF1 inhibitor (pimozide or GW7647) were combined in fixed molar ratios of 1:1 and 1:4. The cell viability was determined in a range of compound concentrations as described above. To calculate the combination index, the dose-response curves were analyzed using CalcuSyn (Biosoft), which is based on the median-effect principle developed by Chou and Talalay (1984). The combination index (CI) was determined for the fraction of cells affected (Fa) following addition of the fixed ratios of cisplatin and USP1/UAF1 inhibitor.

SUPPLEMENTAL INFORMATION

Supplemental Information includes four figures, two tables, and Supplemental Experimental Procedures and can be found with this article online at doi:10.1016/j.chembiol.2011.08.014.

ACKNOWLEDGMENTS

This work was supported in part by a grant from the US National Institute of Health to Z.Z. (Grant R03 DA030552), the Molecular Libraries Program, and the Intramural Research Program of the National Human Genome Research Institute, National Institutes of Health. We thank Zhijiang Yan and Weidong Wang at National Institute on Aging for the protocol of FANCD2 western blot analysis. We also thank Douglas A. Gray and Jan Brun in Ottawa Health Research Institute for the protocol of PCNA western blot analysis.

Received: April 26, 2011
Revised: August 4, 2011
Accepted: August 22, 2011
Published: November 22, 2011

REFERENCES

Adams, J. (2004). The proteasome: a suitable antineoplastic target. Nat. Rev. Cancer *4*, 349–360.

Albertella, M.R., Green, C.M., Lehmann, A.R., and O'Connor, M.J. (2005). A role for polymerase eta in the cellular tolerance to cisplatin-induced damage. Cancer Res. *65*, 9799–9806.

Alpi, A.F., and Patel, K.J. (2009). Monoubiquitylation in the Fanconi anemia DNA damage response pathway. DNA Repair (Amst.) *8*, 430–435.

Amerik, A.Y., and Hochstrasser, M. (2004). Mechanism and function of deubiquitinating enzymes. Biochim. Biophys. Acta *1695*, 189–207.

Amerik, A.Y., Swaminathan, S., Krantz, B.A., Wilkinson, K.D., and Hochstrasser, M. (1997). In vivo disassembly of free polyubiquitin chains by yeast Ubp14 modulates rates of protein degradation by the proteasome. EMBO J. *16*, 4826–4838.

Bergink, S., and Jentsch, S. (2009). Principles of ubiquitin and SUMO modifications in DNA repair. Nature *458*, 461–467.

Bremm, A., Freund, S.M., and Komander, D. (2010). Lys11-linked ubiquitin chains adopt compact conformations and are preferentially hydrolyzed by the deubiquitinase Cezanne. Nat. Struct. Mol. Biol. *17*, 939–947.

Brown, P.J., Stuart, L.W., Hurley, K.P., Lewis, M.C., Winegar, D.A., Wilson, J.G., Wilkison, W.O., Ittoop, O.R., and Willson, T.M. (2001). Identification of a subtype selective human PPARalpha agonist through parallel-array synthesis. Bioorg. Med. Chem. Lett. *11*, 1225–1227.

Brun, J., Chiu, R.K., Wouters, B.G., and Gray, D.A. (2010). Regulation of PCNA polyubiquitination in human cells. BMC Res. Notes *3*, 85.

Chou, T.C. (2010). Drug combination studies and their synergy quantification using the Chou-Talalay method. Cancer Res. *70*, 440–446.

Chou, T.C., and Talalay, P. (1984). Quantitative analysis of dose-effect relationships: the combined effects of multiple drugs or enzyme inhibitors. Adv. Enzyme Regul. *22*, 27–55.

Chou, T.C., Motzer, R.J., Tong, Y., and Bosl, G.J. (1994). Computerized quantitation of synergism and antagonism of taxol, topotecan, and cisplatin against human teratocarcinoma cell growth: a rational approach to clinical protocol design. J. Natl. Cancer Inst. *86*, 1517–1524.

Cohn, M.A., Kee, Y., Haas, W., Gygi, S.P., and D'Andrea, A.D. (2009). UAF1 is a subunit of multiple deubiquitinating enzyme complexes. J. Biol. Chem. *284*, 5343–5351.

Cohn, M.A., Kowal, P., Yang, K., Haas, W., Huang, T.T., Gygi, S.P., and D'Andrea, A.D. (2007). A UAF1-containing multisubunit protein complex regulates the Fanconi anemia pathway. Mol. Cell *28*, 786–797.

Colland, F., Formstecher, E., Jacq, X., Reverdy, C., Planquette, C., Conrath, S., Trouplin, V., Bianchi, J., Aushev, V.N., Camonis, J., et al. (2009). Small-molecule inhibitor of USP7/HAUSP ubiquitin protease stabilizes and activates p53 in cells. Mol. Cancer Ther. *8*, 2286–2295.

Cooper, E.M., Boeke, J.D., and Cohen, R.E. (2010). Specificity of the BRISC deubiquitinating enzyme is not due to selective binding to Lys63-linked polyubiquitin. J. Biol. Chem. *285*, 10344–10352.

Copeland, R.A. (2005). Evaluation of enzyme inhibitors in drug discovery a guide for medicinal chemists and pharmacologists. In Methods of biochemical analysis v 46 (Hoboken, NJ: Wiley-Interscience), pp. 125–128.

Drag, M., and Salvesen, G.S. (2010). Emerging principles in protease-based drug discovery. Nat. Rev. Drug Discov. *9*, 690–701.

Geng, L., Huntoon, C.J., and Karnitz, L.M. (2010). RAD18-mediated ubiquitination of PCNA activates the Fanconi anemia DNA repair network. J. Cell Biol. *191*, 249–257.

Guédat, P., and Colland, F. (2007). Patented small molecule inhibitors in the ubiquitin proteasome system. BMC Biochem. *8* (*Suppl 1*), S14.

Hassiepen, U., Eidhoff, U., Meder, G., Bulber, J.F., Hein, A., Bodendorf, U., Lorthiois, E., and Martoglio, B. (2007). A sensitive fluorescence intensity assay for deubiquitinating proteases using ubiquitin-rhodamine110-glycine as substrate. Anal. Biochem. *371*, 201–207.

Hicks, J.K., Chute, C.L., Paulsen, M.T., Ragland, R.L., Howlett, N.G., Guéranger, Q., Glover, T.W., and Canman, C.E. (2010). Differential roles for DNA polymerases eta, zeta, and REV1 in lesion bypass of intrastrand versus interstrand DNA cross-links. Mol. Cell. Biol. *30*, 1217–1230.

Huang, T.T., Nijman, S.M., Mirchandani, K.D., Galardy, P.J., Cohn, M.A., Haas, W., Gygi, S.P., Ploegh, H.L., Bernards, R., and D'Andrea, A.D. (2006). Regulation of monoubiquitinated PCNA by DUB autocleavage. Nat. Cell Biol. *8*, 339–347.

Inglese, J., Auld, D.S., Jadhav, A., Johnson, R.L., Simeonov, A., Yasgar, A., Zheng, W., and Austin, C.P. (2006). Quantitative high-throughput screening: a titration-based approach that efficiently identifies biological activities in large chemical libraries. Proc. Natl. Acad. Sci. USA *103*, 11473–11478.

Kannouche, P.L., Wing, J., and Lehmann, A.R. (2004). Interaction of human DNA polymerase eta with monoubiquitinated PCNA: a possible mechanism for the polymerase switch in response to DNA damage. Mol. Cell *14*, 491–500.

Kim, J.M., Parmar, K., Huang, M., Weinstock, D.M., Ruit, C.A., Kutok, J.L., and D'Andrea, A.D. (2009). Inactivation of murine Usp1 results in genomic instability and a Fanconi anemia phenotype. Dev. Cell *16*, 314–320.

Kirkin, V., and Dikic, I. (2007). Role of ubiquitin- and Ubl-binding proteins in cell signaling. Curr. Opin. Cell Biol. *19*, 199–205.

Kisselev, A.F., and Goldberg, A.L. (2001). Proteasome inhibitors: from research tools to drug candidates. Chem. Biol. *8*, 739–758.

Kornacker, M.G., Lai, Z., Witmer, M., Ma, J., Hendrick, J., Lee, V.G., Riexinger, D.J., Mapelli, C., Metzler, W., and Copeland, R.A. (2005). An inhibitor binding pocket distinct from the catalytic active site on human beta-APP cleaving enzyme. Biochemistry *44*, 11567–11573.

Lee, B.H., Lee, M.J., Park, S., Oh, D.C., Elsasser, S., Chen, P.C., Gartner, C., Dimova, N., Hanna, J., Gygi, S.P., et al. (2010). Enhancement of proteasome activity by a small-molecule inhibitor of USP14. Nature *467*, 179–184.

McGovern, S.L., Helfand, B.T., Feng, B., and Shoichet, B.K. (2003). A specific mechanism of nonspecific inhibition. J. Med. Chem. *46*, 4265–4272.

Neifeld, J.P., Tormey, D.C., Baker, M.A., Meyskens, F.L., Jr., and Taub, R.N. (1983). Phase II trial of the dopaminergic inhibitor pimozide in previously treated melanoma patients. Cancer Treat. Rep. *67*, 155–157.

Nijman, S.M., Huang, T.T., Dirac, A.M., Brummelkamp, T.R., Kerkhoven, R.M., D'Andrea, A.D., and Bernards, R. (2005a). The deubiquitinating enzyme USP1 regulates the Fanconi anemia pathway. Mol. Cell *17*, 331–339.

Nijman, S.M., Luna-Vargas, M.P., Velds, A., Brummelkamp, T.R., Dirac, A.M., Sixma, T.K., and Bernards, R. (2005b). A genomic and functional inventory of deubiquitinating enzymes. Cell *123*, 773–786.

Oestergaard, V.H., Langevin, F., Kuiken, H.J., Pace, P., Niedzwiedz, W., Simpson, L.J., Ohzeki, M., Takata, M., Sale, J.E., and Patel, K.J. (2007). Deubiquitination of FANCD2 is required for DNA crosslink repair. Mol. Cell *28*, 798–809.

Opler, L.A., and Feinberg, S.S. (1991). The role of pimozide in clinical psychiatry: a review. J. Clin. Psychiatry *52*, 221–233.

Patel, K.J., and Joenje, H. (2007). Fanconi anemia and DNA replication repair. DNA Repair (Amst.) *6*, 885–890.

Radujkovic, A., Schad, M., Topaly, J., Veldwijk, M.R., Laufs, S., Schultheis, B.S., Jauch, A., Melo, J.V., Fruehauf, S., and Zeller, W.J. (2005). Synergistic activity of imatinib and 17-AAG in imatinib-resistant CML cells overexpressing BCR-ABL—inhibition of P-glycoprotein function by 17-AAG. Leukemia *19*, 1198–1206.

Reyes-Turcu, F.E., Ventii, K.H., and Wilkinson, K.D. (2009). Regulation and cellular roles of ubiquitin-specific deubiquitinating enzymes. Annu. Rev. Biochem. *78*, 363–397.

Sato, Y., Yoshikawa, A., Yamagata, A., Mimura, H., Yamashita, M., Ookata, K., Nureki, O., Iwai, K., Komada, M., and Fukai, S. (2008). Structural basis for specific cleavage of Lys 63-linked polyubiquitin chains. Nature *455*, 358–362.

Scheer, J.M., Romanowski, M.J., and Wells, J.A. (2006). A common allosteric site and mechanism in caspases. Proc. Natl. Acad. Sci. USA *103*, 7595–7600.

Shanks, R.H., Rizzieri, D.A., Flowers, J.L., Colvin, O.M., and Adams, D.J. (2005). Preclinical evaluation of gemcitabine combination regimens for application in acute myeloid leukemia. Clin. Cancer Res. *11*, 4225–4233.

Simeonov, A., Jadhav, A., Thomas, C.J., Wang, Y., Huang, R., Southall, N.T., Shinn, P., Smith, J., Austin, C.P., Auld, D.S., and Inglese, J. (2008). Fluorescence spectroscopic profiling of compound libraries. J. Med. Chem. *51*, 2363–2371.

Sonoda, E., Okada, T., Zhao, G.Y., Tateishi, S., Araki, K., Yamaizumi, M., Yagi, T., Verkaik, N.S., van Gent, D.C., Takata, M., and Takeda, S. (2003). Multiple roles of Rev3, the catalytic subunit of polzeta in maintaining genome stability in vertebrates. EMBO J. *22*, 3188–3197.

Southall, N.T., Jadhav, A., Huang, R., Nguyen, T., and Wang, Y. (2009). Enabling the large-scale analysis of quantitative high-throughput screening data. handbook of drug screening. In Handbook of Drug Screening, 2nd ed., R. Seethala and L. Zhang, eds. (New York: Informa Healthcare), pp. 442–464.

Sowa, M.E., Bennett, E.J., Gygi, S.P., and Harper, J.W. (2009). Defining the human deubiquitinating enzyme interaction landscape. Cell *138*, 389–403.

Strobl, J.S., Kirkwood, K.L., Lantz, T.K., Lewine, M.A., Peterson, V.A., and Worley, J.F., 3rd. (1990). Inhibition of human breast cancer cell proliferation in tissue culture by the neuroleptic agents pimozide and thioridazine. Cancer Res. *50*, 5399–5405.

Terai, K., Abbas, T., Jazaeri, A.A., and Dutta, A. (2010). CRL4(Cdt2) E3 ubiquitin ligase monoubiquitinates PCNA to promote translesion DNA synthesis. Mol. Cell *37*, 143–149.

Tian, X., Isamiddinova, N.S., Peroutka, R.J., Goldenberg, S.J., Mattern, M.R., Nicholson, B., and Leach, C. (2011). Characterization of selective ubiquitin and ubiquitin-like protease inhibitors using a fluorescence-based multiplex assay format. Assay Drug Dev. Technol. *9*, 165–173.

Virdee, S., Ye, Y., Nguyen, D.P., Komander, D., and Chin, J.W. (2010). Engineered diubiquitin synthesis reveals Lys29-isopeptide specificity of an OTU deubiquitinase. Nat. Chem. Biol. *6*, 750–757.

Wang, W. (2007). Emergence of a DNA-damage response network consisting of Fanconi anaemia and BRCA proteins. Nat. Rev. Genet. *8*, 735–748.

Wu, F., Lin, X., Okuda, T., and Howell, S.B. (2004). DNA polymerase zeta regulates cisplatin cytotoxicity, mutagenicity, and the rate of development of cisplatin resistance. Cancer Res. *64*, 8029–8035.

Zastre, J., Anantha, M., Ramsay, E., and Bally, M. (2007). Irinotecan-cisplatin interactions assessed in cell-based screening assays: cytotoxicity, drug accumulation and DNA adduct formation in an NSCLC cell line. Cancer Chemother. Pharmacol. *60*, 91–102.

Zeng-Rong, N., Paterson, J., Alpert, L., Tsao, M.S., Viallet, J., and Alaoui-Jamali, M.A. (1995). Elevated DNA repair capacity is associated with intrinsic resistance of lung cancer to chemotherapy. Cancer Res. *55*, 4760–4764.

Zhang, J.H., Chung, T.D., and Oldenburg, K.R. (1999). A simple statistical parameter for use in evaluation and validation of high throughput screening assays. J. Biomol. Screen. *4*, 67–73.

Zhuang, Z., Johnson, R.E., Haracska, L., Prakash, L., Prakash, S., and Benkovic, S.J. (2008). Regulation of polymerase exchange between Poleta and Poldelta by monoubiquitination of PCNA and the movement of DNA polymerase holoenzyme. Proc. Natl. Acad. Sci. USA *105*, 5361–5366.

